thick tassel dwarf1 encodes a putative maize ortholog of the *Arabidopsis CLAVATA1* leucine-rich repeat receptor-like kinase

Peter Bommert[1,*], China Lunde[2], Judith Nardmann[1], Erik Vollbrecht[2,†], Mark Running[2,‡], David Jackson[3], Sarah Hake[2] and Wolfgang Werr[1,§]

[1]Institut für Entwicklungsbiologie, Universität zu Köln, Gyrhofstrasse 17, D-50923 Köln, Germany
[2]Plant Gene Expression Center, Agricultural Research Service – USDA, 800 Buchanan St, Albany, CA 94710, USA
[3]Cold Spring Harbor Laboratory, Cold Spring Harbor, NY 11724, USA

*Present address: Cold Spring Harbor Laboratory, Cold Spring Harbor, NY 11724, USA
†Present address: Department of Genetics, Development and Cell Biology, Iowa State University, Ames, IA 50011, USA
‡Present address: Donald Danforth Plant Science Center, 975 Warson Rd, St Louis, MO 63146, USA
§Author for correspondence (e-mail: werr@uni-koeln.de)

Accepted 17 December 2004

Development 132, 1235-1245
Published by The Company of Biologists 2005
doi:10.1242/dev.01671

Summary

Development in higher plants depends on the activity of meristems, formative regions that continuously initiate new organs at their flanks. Meristems must maintain a balance between stem cell renewal and organ initiation. In fasciated mutants, organ initiation fails to keep pace with meristem proliferation. The *thick tassel dwarf1* (*td1*) mutation of maize affects both male and female inflorescence development. The female inflorescence, which results in the ear, is fasciated, with extra rows of kernels. The male inflorescence, or tassel, shows an increase in spikelet density. Floral meristems are also affected in *td1* mutants; for example, male florets have an increase in stamen number. These results suggest that *td1* functions in the inflorescence to limit meristem size. In addition, *td1* mutants are slightly shorter than normal siblings, indicating that *td1* also plays a role in vegetative development. *td1* encodes a leucine-rich repeat receptor-like kinase (LRR-RLK) that is a putative ortholog of the *Arabidopsis* CLAVATA1 protein. These results complement previous work showing that *fasciated ear2* encodes a CLAVATA2-like protein, and suggest that the CLAVATA signaling pathway is conserved in monocots. *td1* maps in the vicinity of quantitative trait loci that affect seed row number, spikelet density and plant height. We discuss the possible selection pressures on *td1* during maize domestication.

Key words: Meristem, Stem cells, Inflorescence, *thick tassel dwarf1*, Maize

Introduction

Plant growth is characterized by reiterative developmental events that depend upon the activity of meristems. The aerial part of the plant body is elaborated from the shoot apical meristem (SAM), which produces leaves, stems and axillary meristems in a repetitive manner (Galinat and Naylor, 1951; Steeves and Sussex, 1989). Established during embryogenesis, the SAM is self-maintained as a pool of undifferentiated cells during the plant life cycle. A small group of pluripotent stem cells is maintained apically, in the central zone (CZ) of the SAM. Surrounding the CZ is the peripheral zone (PZ), where cells are recruited for elaboration of lateral organs that will form the plant body (reviewed by Kerstetter and Hake, 1997).

Analysis of mutations has identified a few of the genes that control meristem function. One class of mutations is perturbed in meristem formation and/or maintenance. For example, in strong alleles of *shootmeristemless* (*stm*), seedling development stops after formation of the two cotyledons (Barton and Poethig, 1993), whereas analysis of weak *stm* alleles indicates a role for *STM* throughout all stages of shoot meristem development (Clark et al., 1996; Endrizzi et al., 1996). The maize homolog *knotted1* (*kn1*) is also required for shoot meristem establishment and maintenance (Kerstetter et al., 1997; Vollbrecht et al., 2000). The *kn1* and *STM* homeobox genes are expressed throughout the SAM, except in the cells that are destined to become the next leaf primordium (Smith et al., 1992; Jackson et al., 1994; Long et al., 1996). Plants carrying loss-of-function mutations at the *WUSCHEL* (*WUS*) locus also fail to maintain the SAM (Laux et al., 1996). *WUS* encodes a novel subtype of homeodomain protein that is nuclear localized and predicted to act as a transcription factor (Mayer et al., 1998). *WUS* mRNA is first detected when embryos reach the 16-cell stage and becomes localized to a group of cells that underlies the presumptive stem cells, suggesting that it may act in promoting stem cell fate non-autonomously.

A second class of mutations displays meristem enlargement, which can lead to fasciation in extreme cases. Fasciation, derived from the Latin word *fascis*, meaning ‘bundle’, is a reflection of increased proliferation. Fasciated variants are reported to have increased crop yields, for instance by increasing fruit size in tomato (Luckwill, 1943; Zielinski, 1945). Fasciation also has a long history of study in maize (Emerson, 1912): *Fascicled ear1* (*Fas1*), *fasciated ear1* (*fea1*), *fasciated ear2* (*fea2*) and *thick tassel dwarf1* (*td1*) are

characterized by a fasciated ear morphology (Orr et al., 1997; Jackson and Hake, 1999).

In *Arabidopsis*, mutations in the three *CLAVATA* loci (*CLV1*, *CLV2* and *CLV3*) result in a phenotype opposite to that of *wus* and *stm* (Clark et al., 1993; Clark et al., 1995; Kayes and Clark, 1998). The embryonic SAM of *clv*-mutants is slightly larger than that of wild-type embryos. During postembryonic growth, the SAM gradually increases in size, resulting in altered phyllotaxy and supernumerary floral organs. These mutant phenotypes indicate a role for the *CLV* genes in restricting the size of the stem cell population. All three *CLV* genes have been identified and their protein products probably constitute a single receptor-ligand complex, consistent with the three mutants having an almost identical phenotype (Clark et al., 1997; Fletcher et al., 1999; Jeong et al., 1999). The CLV1 protein is a receptor-like kinase composed of a leucine-rich repeat-containing extracellular domain with putative receptor function and a cytoplasmic Ser/Thr kinase domain linked through a transmembrane domain (Clark et al., 1997). CLV2 is structurally similar to CLV1 but lacks a cytoplasmic kinase domain (Jeong et al., 1999). *CLV3* encodes a 96 amino acid polypeptide that contains a putative signal sequence and is secreted (Rojo et al., 2002). *CLV3* transcripts are preferentially found in the outer L1 and L2 layers, whereas *CLV1* is expressed specifically in the L2 and L3 layers of the SAM. *CLV2* is expressed ubiquitously (Jeong et al., 1999). The *WUS* and *CLV* pathways are interdependent (Brand et al., 2000; Schoof et al., 2000); *WUS* promotes stem cell fate, whereas CLV signaling restricts the number of stem cells (reviewed by Sharma et al., 2003a).

The maize ear comprises a series of meristem types (reviewed by McSteen et al., 2000) and changes in meristem size and identity may underlie the yield increases brought about during the domestication of maize (Kellogg and Birchler, 1993) from teosinte inflorescences (Beadle, 1980; Doebley, 1992). Whereas seeds are arranged in single alternating rows in teosinte, present-day maize lines have a polystichous arrangement of seeds consisting of 8 to 18 rows, and in some varieties up to 36 rows (USDA, ARS, National Genetic Resources Program, Germplasm Resources Information Network; http://www.ars-grin.gov/cgi-bin/npgs/). The increased number of axillary meristems in maize is thus a major acquired character, which has been instrumental in the domestication of maize as a crop plant. It would be of interest to understand how ear size relates to the stem cell concept and reflects modulations in the size of the stem cell population, since the increase in seed row number of the maize ear is reminiscent of supernumerary lateral organs that arise due to increased meristem size in *clv* mutants.

The maize *fea2* locus encodes a potential ortholog of *CLV2*, suggesting that the *CLAVATA* pathway is functionally conserved in monocot species and acts to limit size or growth of meristems during maize development (Taguchi-Shiobara et al., 2001). Further evidence comes from the recent characterization of the *FON1* gene in rice, which encodes a potential *CLV1* ortholog (Suzaki et al., 2004). As in *clv1* mutants, *fon1* mutant plants produce enlarged floral meristems and additional floral organs. By contrast to *clv1* mutants, however, *fon1* mutants do not have significantly enlarged vegetative shoot or inflorescence meristems.

Considering that maize was domesticated at least 6000 years ago (Piperno and Flannery, 2001), the unique monstrosity of the maize ear in the plant kingdom could reflect permanent selection for size increase of the ear inflorescence meristem, which is still a major quantitative trait of interest in modern maize breeding. We are now in a position to ask whether modifications of specific signaling pathways, such as the CLV pathway, may have contributed to the domestication of crop plants. Here we describe a reverse genetics approach to functionally characterize *CLV1* homologs from maize. The maize gene most similar to *CLV1* encodes *thick tassel dwarf1* (*td1*). The fasciation phenotype of *td1* mutant alleles provides further evidence that meristem size in maize is controlled by the CLV signaling pathway. However, significant qualitative and quantitative differences exist between the *td1* and *CLV1* expression patterns. These differences emphasize that it is important to study developmental processes in agronomic crops such as maize, as well as in model species such as *Arabidopsis*.

Materials and methods

Genetics

The *glassfingers* (*glf*) mutation (now called *td1-glf*) was mapped using waxy translocations to chromosome 5S. Complementation crosses with *td1-Ref* (obtained from the Maize Genetics Cooperative Stock Center) confirmed allelism. Both *td1-glf* and *td1-Ref* were introgressed into B73 and W22 for phenotypic observations. Additional alleles (see Table 1) were obtained by crossing *td1-Ref* or *td1-glf* homozygotes as males onto *Mutator* stocks. Screens were carried out in Davis, California and in Illinois. *td1-mum3* was identified in a F2 family of the Maize Gene Discovery Project (Lunde et al., 2003). A F2 family segregating for *fea2*, *td1* double mutants was created by crossing individuals homozygous for *fea2-O* and *td1-glf* respectively, and selfing the resulting progeny. Both mutations were in the B73 background.

Isolation of the full-length *ZmKin5* gene

By using the degenerate primers (5′-GG5 AAR GGM GGM GC5 GGR ATY GTS TA-3′; 5′-TTR GCR AGS CCR AAR TCR GCR AC-3′), and genomic DNA as a template, five *CLV1* related kinase sequences, designated as *ZmKin1* to *5*, have been isolated. A cDNA library constructed in Zap II (Stratagene) using mRNA from leaf-stage 4 embryos [staged according to Abbe and Stein (Abbe and Stein, 1954)] was screened using individual *ZmKin5* specific 5′-biotinylated forward and reverse primers (5′-GTTGGAGACAAGCCGAGCAG-3′, 5′-GCCGCACCCTCTCCCCACCAG-3′) in linear PCR. PCR products from these reactions were purified using Dynabeads according to the manufacturer's instructions (DYNAL) and amplified exponentially with nested *ZmKin5* primers and vector-specific primers. This cDNA-based strategy yielded partial sequence information extending from the last extracellular LRR-repeat through the kinase domain to the stop codon, plus sequences of the 3′ untranslated region (UTR) to the poly-A tail. To obtain the full length *ZmKin5* sequence, a genomic library of genotype HD5 × HD7 in vector EMBL3 SP6/T7 (Clontech) was screened with a ^{32}P-labeled *ZmKin5* fragment representing 450 bp of the less conserved carboxy terminal part of the kinase domain plus 170 bp of the 3′ UTR. Genomic maize DNA from positive plaques was isolated and cloned into pBluescript II SK (Stratagene) and sequenced.

td1 expression analysis

Maize tissues were ground to a fine powder in liquid nitrogen and RNA was purified using the Trizol procedure (Invitrogen). PolyA$^{(+)}$ RNA was isolated using oligo-dT cellulose columns or a Dynabeads mRNA purification kit (DYNAL). RNA electrophoresis, transfer to a

Hybond-N membrane (Amersham Pharmacia Biotech) or Magna, nylon membrane (Osmonics) and hybridizations followed the protocol of Smith et al. (Smith et al., 1992). Hybridization with the ^{32}P-labeled 620 bp probe (450 bp of kinase coding sequence + 170 bp 3′ UTR) was performed at 42°C overnight. Blots were washed in 0.1 × SSC, 0.1% SDS at 65°C and autoradiographed on Kodak X-omat AR films or by visualization on a PhosphorImager (Molecular Dynamics).

For real-time PCR analysis, tissue-specific cDNAs were synthesized using the SuperScriptIII™ reverse transcriptase according to the manufacturer's instructions (Invitrogen). Real-time RT-PCR analysis was performed on a GeneAmp® 5700 Light Cycler. The *on-line* detection of amplification rates was performed using SYBR® Green (Applied Biosystems). Normalization was performed against *Ubiquitin* with primers: UBI-Fo (5′-TAAGCTGCCGATGTGCCT-GCG-3′) and UBI-Re (5′-CTGAAAGACAGAACATAATGA-GCACAG-3′). *Knotted1*-specific amplicons were generated with primers: kn1-Fo (5′-ACCGAGCTCCCTGAAGTTGATG-3′) and kn1-Re (5′-CTAGGCCGTGGGGTGTGAAATGC-3′). The *td1*-specific primers were: td1-Ref-Fo (5′-GCTGCTGGCGGACCTCTA-CA-3′) and td1-Ref-Re (5′-GACGAGTGACGCCAAAAAG-3′).

Female and male inflorescences for in-situ hybridizations were dissected and fixed at 4°C overnight in 4% formaldehyde with 0.1% TritonX100 (Sigma) in PBS, dehydrated in an ethanol series, cleared in Histoclear (Roth) and embedded in paraffin wax (Paraplast plus, SIGMA). Sections 7-9 μm thick were mounted on coated slides (SuperFrost®Plus). The *td1* probe (620 bp, see above) was cloned into pBluescript II SK (Stratagene). The *td1* and the *kn1* probes (Jackson et al., 1994) were labeled by incorporation of digoxigenin-UTP (Roche) during SP6/T3 transcription. RNA in-situ hybridization was performed according to the method of Jackson et al. (Jackson et al., 1994).

Scanning electron microscopy

Scanning electron microscopy was performed according to the protocol outlined in Sommer et al. (Sommer et al., 1990) and images were processed digitally.

PCR on *td1* alleles and double mutant families

Genomic DNAs of homozygous *td1-Ref* and *td1-Nickerson* plants were used as templates in PCR reactions with primers 5′-CATGCCACCTGCCTTTGAC-3′ and 5′-GACGAGTGACGCCA-AAAAG-3′ and Platinum Pfx proofreading polymerase (Invitrogen) or Fisher Taq polymerase. DNA sequence analysis followed cloning into the pCR2.1-TOPO vector (Invitrogen) or pGemT-EZ vector (Promega).

The *Mu*-alleles were amplified using platinum Pfx proofreading polymerase (Invitrogen) using forward or reverse *td1*-primers ~500 bp apart and covering the entire coding region, and *Mu*-specific primers (5′-GCCTCCATTTCGTCGAATC-3′ or Pioneer's 9242 *Mu*-specific primer 5′-AGAGAAGCCAACGCCAWCGCCTCYATTTCGTC-3′) (Blauth et al., 2001) located in the terminal inverted repeat sequences of the transposable element. The resulting amplicons were cloned and sequenced to determine the *Mu*-insertion site.

Genotypes of individuals in the segregating F2 families used for double mutant analysis were determined by using primers specific to *fea2* (fea2-Fo: 5′-GCTGCTGGCGGACCTCTACA-3′; fea2-Re: 5′-GACGAGTGACGCCAAAAAG-3′) or *td1* (td1-Fo: 5′-TCACCG-ACAACATGCTCACT-3′; td1-Re: 5′-CAAACACGTGGTTATG-CTGC-3′) and the 9242 primer. Wild-type chromosomes were detected by amplifying with gene-specific primers flanking the known *Mu* insertion sites in each allele.

Results

td1 mutant phenotype

Maize, a monoecious plant, develops distinct male and female inflorescence structures. The terminal shoot apical meristem gives rise to the tassel, the male inflorescence, whereas axillary meristems, initiated in leaf axils, produce the female inflorescences, or ears. The recessive *thick tassel dwarf1* allele (*td1-ref*) was first reported by E. G. Anderson and has been donated to the MGC stock center (M. Sachs, personal communication). *td1* mutants are fertile, and the most pronounced phenotypic alterations are detected in the inflorescences, although plants are also noticeably shorter in some inbred backgrounds.

The mature tassel of maize consists of a central rachis and a few long branches at the base, with each axis lined with rows of spikelets. In the tassel of *td1* mutant plants, the main rachis was thicker than normal, and this was more obvious when spikelets were removed (Fig. 1A,B). This increase in rachis diameter was reflected in a higher spikelet density. Whereas normal sibling tassels on average produced around 14 spikelets/cm on the main rachis, *td1* mutant tassels could produce more than 20 spikelets/cm (Table 2). This increase in spikelet density was proportionally similar in tassel branches (Table 2). However, the total number of spikelets per tassel was not always increased, as thickening of the main axis in *td1* tassels was sometimes correlated with a reduction in length (Table 2). The spikelets are arranged in pairs, with a pedicellate and sessile spikelet (Fig. 1E). Male spikelets contain two glumes that surround two florets. Each floret contains three stamens, two lodicules and an aborted pistil (Cheng et al., 1983). A closer inspection of male spikelets in *td1* mutants showed a high frequency of single spikelets instead of paired spikelets (Fig. 1C; Table 2). The spikelets themselves were occasionally irregular, with extra glumes (Fig. 1C), and florets often contained more than three stamens (Fig. 1D; Table 2). These supernumerary floral organs may have resulted from an enlarged floral meristem.

Development of the ear was also significantly altered in *td1* mutants. During normal ear development, the inflorescence meristem (IM) initiated spikelet pair meristems (SPMs) in a

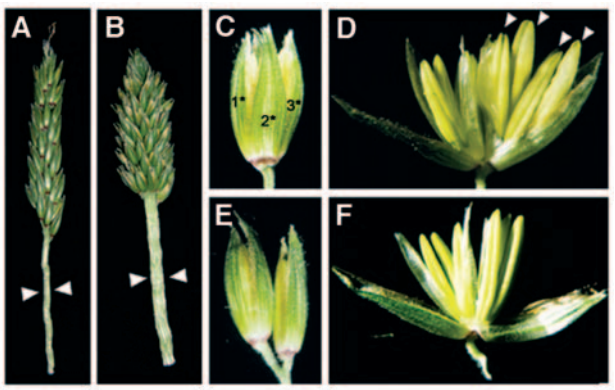

Fig. 1. Tassel development in *td1* mutants. (A) Tassel rachis of normal sibling with some spikelets removed at the base. (B) Tassel rachis of *td1-Ref* mutant with spikelets removed. (C) A single spikelet of *td1-Ref* with three glumes (numbered). (D) *td1-Ref* spikelet with two florets, one of which contains four stamens (arrowed). (E) Paired spikelets from a normal tassel. (F) Normal spikelet opened to reveal two florets, each with three stamens. Images are from *td1-Ref* introgressed into W22 and the normal siblings in an F2 family.

Table 1. Source and molecular lesions of *td1*-alleles

Allele	Source	bp of insertion (relative to ATG)/defect
td1-Ref/td1-nickerson	Maize Genetics Stock center	Deletion of amino acids 15-19; substitution of amino acids 9, 12, 21 and 24
td1-mum1	Targeted tagging with *Mu*	*Mu* element insertion +230 bp; in exon 1
td1-mum2	Targeted tagging with *Mu*	*Mu* element insertion +1526 bp; in exon 1
td1-mum3	Non-targeted tagging with *Mu* (MGDP*)	*Mu* element insertion +1860 bp; in exon 1
td1-mum4	Targeted tagging with *Mu*	*Mu* element insertion +2290 bp; in exon 1
td1-mum5	Targeted tagging with *Mu*	*Mu* element insertion +2644 bp; in intron
td1-glf	Non-targeted tagging with *Mu* (S.Briggs, Pioneer)	Deletion of amino acids 15-19; substitution of amino acids 9, 12,21, 24 and *Mu* element insertion +1900 bp; in exon 1

MGDP*, Maize Gene Discovery Project.
Base pair numbers are relative to predicted start codon.

Table 2. Tassel characteristics and plant height in *td1* mutants and normal sibs

Genotype	Spikelet density of rachis*	Spikelet density of branch†	Single spikelets‡/ total spikelets	Stamen number (cm)	Rachis length§ (cm)	Plant height (cm)	Leaf number
td1-Ref	21.0 (4.4; 8)	6.3 (1.5; 8)	0.60 (0.39) 3¶	3.8 (0.6; 3)	20.1 (1.8; 8¶)	35.9 (5.6; 8)	15.8 (0.7; 8)
N sibs	13.8 (3.1; 14)	4.4 (0.9; 14)	0.01 (0.01) 3	3.0 (0.1; 3)	20.8 (2.9; 14)	41.8 (5.2; 14)	18.6 (1.3; 24)
td1-glf	16.2 (2.2; 7)	5.7 (1.8; 7¶)	nd	nd	16.3 (2.6; 7)	137.9 (28.5; 7)	19.0 (0; 6)
B73	14.1 (2.2; 12)	5.2 (0.9; 12)	nd	nd	20.8 (2.8; 12)	171.8 (25.2; 12)	21.9 (0.3; 30)

Numbers are mean values, with standard deviations in parentheses, followed by the number of individuals measured. *td1-Ref* mutants were backcrossed to W22 three times and normal sibs were used for comparison. *td1-glf* mutants were backcrossed to B73 nine times, B73 was used for comparison. Data were collected from plants grown at Gill Tract, Albany, CA in summer 2003, except that leaf number and plant height were collected from seeds of the same cross, planted in the greenhouse in fall of 2004.

*Number of spikelets per cm on central spike of mature tassel, 4 cm were counted after 2 cm were removed from the tip.

†Number of spikelets per cm on lowest tassel branch, 4 cm were counted after 2 cm were removed from the tip.

‡Ratio of number of single spikelets to number of total spikelets on rachis of mature tassel, 4 cm were counted after 2 cm were removed from the tip.

§Length of main spike from the tip to the first long tassel branch.

¶Values for *td1* and normal sibs are significantly different ($P<0.05$), except for ratio of single spikelets to total spikelets ($n=6$, $P=0.12$) and mean rachis length in the *td1-Ref*/W22 ($P=0.49$) family and branch spikelet density in the *td1-glf*/B73 family ($P=0.51$).

nd, no data.

regular phyllotaxy and the SPMs later branched to generate a pair of spikelet meristems (SMs) that were aligned in adjacent vertical rows, which corresponded to rows of seeds in the mature cob (Fig. 2A,B). Mutant *td1* ears were fasciated and wider than corresponding wild-type ears (Fig. 2A). The consequences varied among siblings; in some cases, enlargement of the IM led to a ridge-like structure (Fig. 2C). In other cases, the IM was bifurcated, as shown in Fig. 2D, which resulted in branched ears at maturity, or showed ring fasciation (Fig. 7B).

In *td1* mutant ears, supernumerary rows of spikelets were often interspersed among more normally developed rows, and did not extend to the base of the ear as did all rows in wild-type ears (Fig. 2D). These additional rows coincided with flattening and enlargement of the IM, which became progressively more severe during ear development, leading to the initiation of up to ~54 rows of seeds compared with ~16 in normal siblings (Table 3). Differences in ear development were not confined to the IM but were also detected in the SPM and SM. In *td1* mutant ears, the regular arrangement of SPMs was disturbed (Fig. 2D). Single SPMs were enlarged, and both the timing and the orientation of SPM branching were uneven compared with wild type. SPMs normally gave rise to a pair of SMs in wild type (Fig. 2B); by contrast, clusters of three SMs could be detected in *td1* ears (Fig. 2E), and some SMs were enlarged (Fig. 2F). Supernumerary SMs originating from a single SPM were consistent with meristem enlargement, although we have not statistically compared SPM size between normal and *td1* ears. The *td1* mutation also affected the vegetative phase of development. *td1-Ref* and *td1-glf* mutants were shorter than normal siblings and produced fewer leaves (Table 2). Time to flower did not appear to be affected (data not shown).

In order to identify meristematic tissues in the aberrantly developed IMs in *td1* mutant ears, sections were hybridized in situ with a *knotted1* (*kn1*) antisense probe (Jackson et al., 1994). As in wild type, *td1* mutant ears strongly expressed *kn1* in the entire apical region, indicating normal shoot meristem identity (compare Fig. 2G and H).

In summary, loss of *td1* activity in the tassel caused thickening of the rachis, a higher spikelet density and extra glumes and stamens. The phenotype was more pronounced in the ear, where fasciation and bifurcation of the IM was accompanied by supernumerary and larger SPMs that branched to produce clusters of SMs of abnormal size. Additionally, a weak vegetative phenotype could be observed in *td1* mutant plants. These phenotypes are all consistent with the observation that *td1* functions to limit meristem size.

Isolation of *CLAVATA1* homologous genes from maize

Like most eukaryotic protein kinases, leucine-rich repeat receptor-like kinases (LRR-RLKs) share 12 highly conserved subdomains within their intracellular catalytic kinase domains. These subdomains have been designated I-XII (Hanks and Quinn, 1991) and invariant amino acid residues in individual subdomains provide excellent anchor points to design degenerated PCR primers. Based on invariant amino acids in subdomains I and VII and guided by flanking sequences in *CLV1* (GI: 15222877), and its closest relatives in the

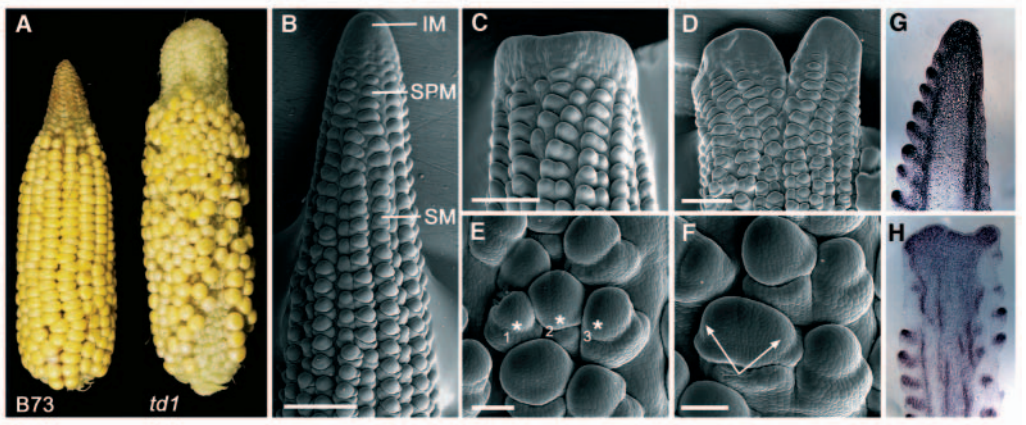

Fig. 2. Ear development in *td1* mutants. (A) Comparison of normal (left) and *td1-Ref* ear (right) at 20 days after pollination. (B) Scanning electron micrograph (SEM) of normal ear. (C-F) SEMs of *td1* mutant ears. The regular arrangement of the SPMs is disturbed, especially at the tip of the ear. Occasionally, SPMs give rise to three SMs (E, numbered asterisks). SPMs are frequently larger than normal (F; arrows). (G) In-situ hybridization with *kn1* on normal ear or (H) *td1-Ref* ear. Scale bars: 500 μm in B,C,E; 100 μm in D,F.

Table 3. Ear spikelet number and leaf number in segregating *td1-glf/ fea2-Ref* double mutant families

Genotype	Number of spikelets*	Leaf number†
td1/td1; fea2/fea2	123.5 (23.3; 2)	14.8 (1.1; 5)
+/+; fea2/fea2	68.5 (22.4; 6)	17.8 (1.0; 6)
td1/td1; +/+	53.7 (16.7; 6)	17.8 (0.8; 6)
td1/+; fea2/+	15.4 (1.9; 15)	19.8 (0.7; 10)
+/+; +/+	15.5 (1.5; 14)	19.6 (1.0; 7)

Numbers are mean values, with standard deviations in parentheses, followed by the number of individuals measured.
*Number of spikelets were counted from a cross-section of the ear at the widest point. Data are combined for plants grown in the field and greenhouse.
†Values are from plants grown in the greenhouse.

Arabidopsis or rice genomes (GI: 15239123 and GI: 18855025) respectively, PCR primers were designed (for sequences see Materials and methods). The relative position of these primers in the kinase domain of *CLV1* are indicated in Fig. 3A.

These primers amplified five *CLV1*-like kinase sequences from genomic maize DNA, which we designated *ZmKin1-5*. To estimate phylogenetic relationships, we extracted highly related LRR-RLK sequences from the National Center for Biotechnology Information (NCBI; http://www3.ncbi.nlm.nih.gov) or DNA Data Bank of Japan (DDBJ; http://www.ddbj.nig.ac.jp/) databases. The *CLUSTALW* program was used to align the kinase domain sequences and estimation of the phylogenetic relationships was performed with the *Minimum Evolution* algorithm provided by the MEGA2.1 software (Kumar et al., 2001). The resulting phylogenetic tree is depicted in Fig. 3B and shows two distinct *CLV1*-like subfamilies, which we call subfamily A and B, substantiated by high bootstrap values. *CLV1* is in a distinct branch of subfamily A, separated from other dicot sequences. Two monocot genes, the maize *Kin5* and the rice *CLV1* ortholog *FON1* (Suzaki et al., 2004), are also found within subfamily A.

Three other maize kinases, *ZmKin1-3*, fall into subfamily B, which also splits into monocot and dicot clades. This splitting validates the phylogenetic reconstruction and suggests that a common ancestral gene may have duplicated to give rise to two separate lineages of LRR-RLK genes prior to the divergence of monocots and dicots. We used the more distantly related *ZmKin4* to root the tree. This phylogeny

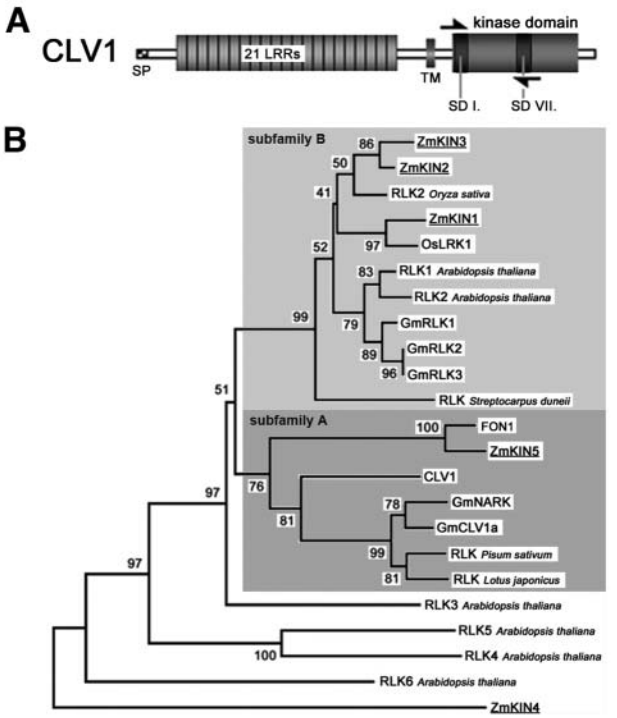

Fig. 3. The CLAVATA1 protein and phylogeny. (A) Schematic of predicted domains in the CLV1 protein. The 21 LRR-motifs are indicated in gray, the kinase domain is depicted in orange; SP: signal peptide; TM: transmembrane domain. Black arrows indicate the position of the degenerate primers. (B) Phylogenetic analysis with LRR-RLK sequences obtained from NCBI or DDBJ databases. The kinase domain sequences were aligned using the *CLUSTALW* program (http://www.ebi.ac.uk/clustalw/-index.html). The phylogenetic reconstruction was performed with the *Minimum Evolution* algorithm provided by the MEGA2.1 software (Kumar et al., 2001). The tree indicates the existence of two closely related *CLV1*-like subfamilies, including the newly isolated maize sequences *ZmKin1*, *2*, *3 and 5*. *Arabidopsis thaliana*: CLV1 gi:15222877, RLK1 gi:30698151, RLK2 gi:15229189, RLK3 gi:15235366, RLK4 gi:15225805, RLK5 gi:15220056; *Oryza sativa*: OsLRK1 gi:8132685, FON1 AB182388, RLK2 gi:34915202 *Glycine max*: GmRLK1 gi:9651941, GmRLK2 gi:9651943, GmRLK3 gi:9651945, GmClv1a gi:11260266, GmNARK gi:25732530; *Pisum sativum*: RLK gi:24940244; *Lotus japonicus*: RLK gi:24940156; *Streptocarpus dunelii*: RLK AY061836.

identified *ZmKin5* as the most likely maize ortholog of *CLV1* from *Arabidopsis*.

ZmKin5 gene structure

To isolate the full-length *ZmKin5* coding sequence, we screened a maize embryo cDNA library with PCR primers from the kinase domain and the vector. Although successful for the 3′ end of the gene, this strategy failed for the 5′ end. We therefore isolated a *ZmKin5* genomic clone by screening with a *ZmKin5*-specific probe comprised of the carboxy terminus of the kinase domain and 3′ UTR sequences. Analysis of the genomic clone indicated that the predicted *ZmKin5* open reading frame is 2991 bp in length. The predicted size of 3262 bp from the ATG translation start codon to the polyA tail was consistent with a single ~3.4 kb transcript detected in RNA gel blot experiments (Fig. 5A). A single intron in the kinase domain was conserved in position in *ZmKin5* and *CLV1*. The amino terminal leucine-rich repeat coding sequences and transmembrane domains were devoid of intervening sequences in maize, as in *Arabidopsis*. The predicted protein sequences encoded by *ZmKIN5* and *CLV1* are compared in Fig. 4A.

Motif searching using the SMART algorithm (http://smart.embl-heidelberg.de/) predicted a hydrophobic 26 amino acid residue ER targeting signal peptide at the amino terminus, which according to the TargetP cleavage site prediction program (http://www.cbs.dtu.dk/services/TargetP/) may be processed. This signal peptide is followed by 21 tandem copies of 23-25 amino acid residue long leucine-rich repeats (LRRs) that, as in CLV1, are flanked by pairs of spaced cysteines. According to the classification of Shiu and Bleeker

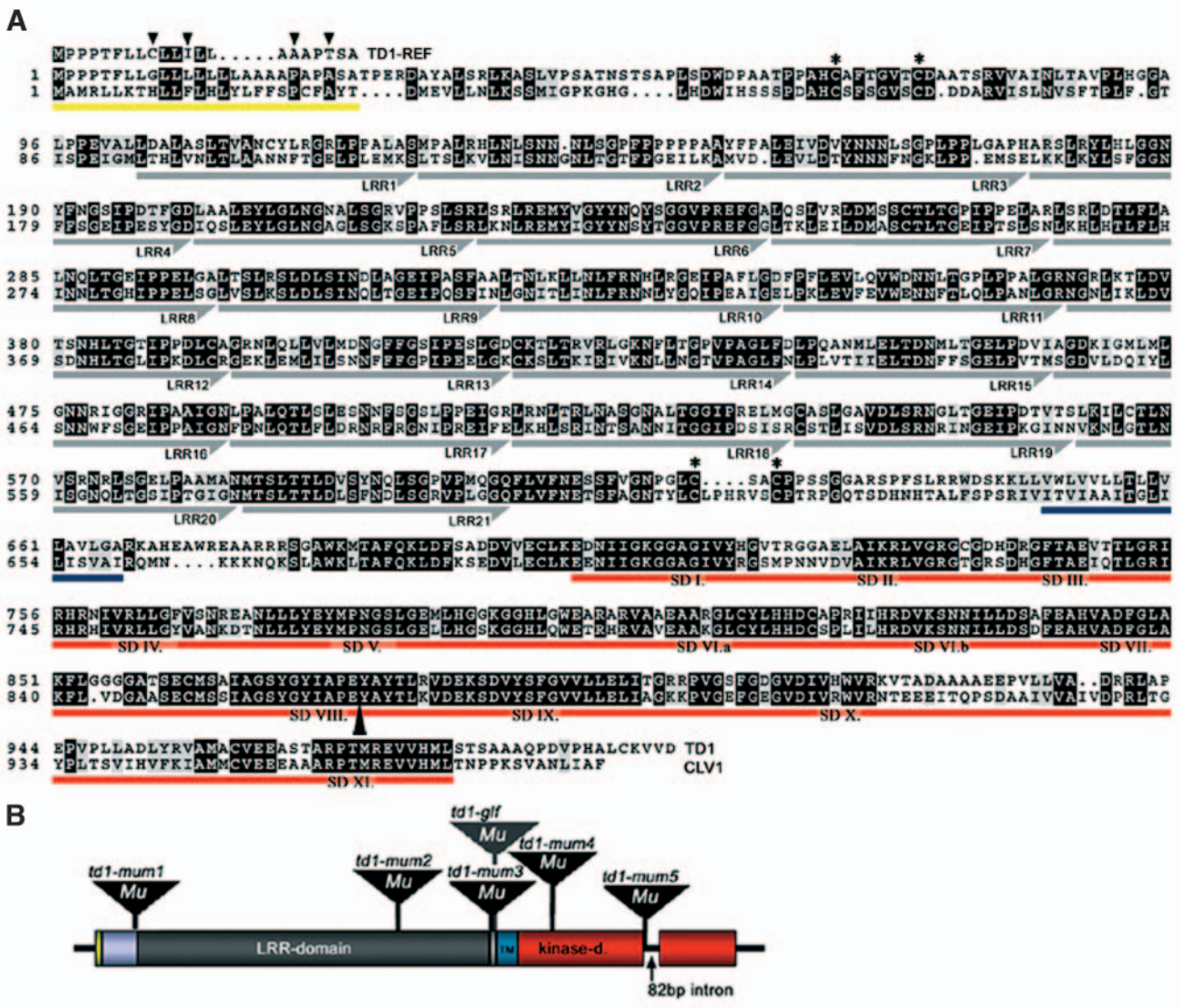

Fig. 4. Molecular characterization of *td1*. (A) *CLUSTALW* alignment of TD1 (from B73 inbred line; top line) and CLV1 (below, GenBank Accession No.: 15222877). Identical residues are outlined in black, similar in gray; dashes represent gaps introduced to optimize the alignment. The black arrow indicates the position of the single intron. Predictions of transmembrane and signal sequences are by SMART (http://smart.embl-heidelberg.de/) for TD1 and from Clark et al. (Clark et al., 1997) for CLV1. Domains are labeled below the respective sequences; yellow, signal peptide; gray, extracellular LRR domain, numbering of single LRR motifs; blue, transmembrane domain; red, kinase domain (the 12 subdomains are labeled SDI-SDXII). Cysteine pairs are marked by asterisks above the respective sequences. The defect in the polypeptide encoded by *td1-Ref* is shown above TD1. (B) Schematic representation of the *Mu* element insertion sites within the different *td1* alleles.

(Shiu and Bleeker, 2001), both 21 LRR motifs of ZmKIN5 and CLV1 belong to the LRR-XI subfamily of LRR motifs. The LRR domain is followed by a predicted transmembrane domain (ZmKIN5 residues 648-665). The intracellular kinase domain comprises the characteristic 12 subdomains with all invariant amino acid residues conserved in comparison to other eukaryotic protein kinases (Hanks and Quinn, 1991) (Fig. 4A). Conserved motifs in subdomains VIb (HRDVKSNN) and VIII (GSYGYIAPEY) predict ZmKIN5 functions as a serine/threonine protein kinase (Fig. 4A). Amino acid similarity and identity to CLV1 are 79 and 72%, respectively, within the kinase domain and 66 and 58%, respectively, over the entire predicted proteins.

ZmKin5 is encoded by the *td1* locus

We mapped *ZmKin5* using the BNL T232/CM37 recombinant inbred lines (Burr et al., 1988) to chromosome 5 (bin 5.03) between markers uaz77 and ici287, close to the *td1* locus. To test the relationship between *ZmKin5* and *td1*, we isolated and sequenced *ZmKin5* genomic DNA from homozygous *td1-Ref* plants. The *td1-Ref* allele harbors a cluster of four base pair substitutions surrounding a 15 bp deletion in the predicted ER targeting signal sequence (Fig. 4A). This mutation is predicted to abolish ER targeting of the protein by the target algorithm. Altered localization of the ZmKIN5 receptor kinase might explain the *td1-Ref* mutant phenotype. The same sequence differences within the putative ER targeting signal were found in the *td1-Nickerson* allele, although both *td1* alleles have been maintained as distinct mutations in the Maize Stock Center, and are believed to have arisen independently (M. Sachs, personal communication). Our data indicate, however, that both mutations may share a common origin.

To determine whether or not *ZmKin5* corresponded to the *td1* locus, we generated additional *td1* mutant alleles. *td1-Ref* and *td1-glf* were crossed as males onto *Mutator* (Robertson, 1978) plants and the resulting progeny were screened for the *td1* mutant phenotype. Twelve putative mutant *td1* alleles were found from screens of approximately 150,000 plants. DNA from putative new alleles was analyzed by PCR for the presence of *Mu* elements in the *ZmKin5* sequence (see Materials and methods). Among 12 alleles examined, five *Mu* insertion alleles were identified, referred to as *td1-mum1* to *-mum5* (Table 1; Fig. 4B). Sequencing of the PCR amplicons revealed *Mu* insertions in the first exon, disrupting the extracellular LRR domain for *td1-mum1*, *td1-mum2* and *td1-mum3*. The *Mu* element in *td1-mum4* was located within the intracellular kinase domain, and in *td1-mum5* was 29 bp downstream of the splice donor site in the single intron. We also found that the *td1-glf* allele had a *Mu* insertion in the first exon. This allele also carried the same polymorphisms as the *td1-Ref* allele within the putative ER targeting signal sequence. Southern hybridizations confirmed co-segregation of a *ZmKin5*-specific *Mu* insertion with the *td1* mutant phenotype in over 40 chromosomes (data not shown). In conclusion, six independently isolated *td1* alleles were shown to contain *Mutator* element insertions in the *ZmKin5* coding region, demonstrating that *ZmKin5* corresponds to the *td1* gene.

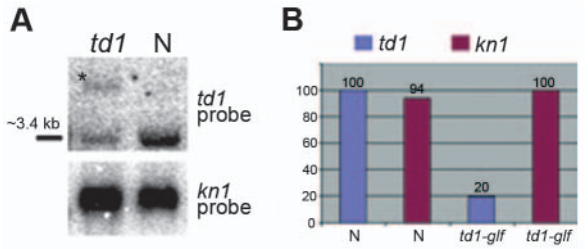

Fig. 5. *td1* transcripts are decreased in a *td1-Mu* allele. (A) RNA gel blot of 2 μg polyA$^{(+)}$ RNA from immature ears of *td1-glf* and normal siblings was hybridized to a *td1* specific probe and revealed an abnormal sized transcript (asterisk). The same membrane was stripped and re-probed with the *kn1* cDNA as a loading control. (B) Real-time RT-PCR also showed that the level of *td1* RNA was reduced in *td1-glf* (20%) relative to wild type, whereas the level of the *kn1* meristem marker was slightly increased.

We also compared *td1* transcript levels in immature ears of normal siblings and *td1-glf* homozygous mutant plants by RNA gel blot experiments. As shown in Fig. 5A, a larger, aberrant transcript was detected using a *td1*-specific probe in RNA from the *td1-glf* mutant. Additionally, real-time RT-PCR showed that the level of *td1* RNA in *td1-glf* was reduced to 20% that of wild type, whereas the level of the *kn1* meristem marker was slightly increased (Fig. 5B). This increase in *kn1* RNA may reflect an increase in IM size or the presence of supernumerary SPMs. Sequence analysis of an RT-PCR product from *td1-glf* RNA revealed the presence of 180 nucleotides of the *Mu* terminal inverted repeat, which would lead to a frame shift and premature translation stop in the extracellular LRR domain. These results demonstrate that the *Mu* element insertion in *td1-glf* is spliced out incompletely, and that *td1-glf* may represent a null allele. In summary, by identifying five independent *td1 Mu*-alleles, we have shown that *td1* is *ZmKin5*, a maize ortholog of *CLV1*.

Expression pattern of the *td1* gene

Organ specificity of *td1* transcription was determined via RNA gel blot hybridizations (data not shown) and quantified by real-time RT-PCR analysis (Fig. 6A). Normalized to *ubiquitin* transcript levels, the highest *td1* transcript level was detected in the apex of the vegetative seedling, and was arbitrarily set at 100%. The RNA level was lower in the ear (58%) and tassel (data not shown). Low *td1* transcript levels were detected in the embryo (11%) and root (11%). In contrast to *CLV1* (Clark et al., 1997), a significant *td1* transcript level was detected in young leaves (63%). Primer specificity for *td1* was verified by direct sequencing of the PCR amplicons.

To analyze the expression pattern of *td1* RNA at a finer resolution, in-situ hybridization experiments were performed with a *td1*-specific probe corresponding to the carboxy terminus of the kinase domain and 170 bp of the 3′ UTR. *td1* transcripts were detected in the vegetative shoot apex in leaf primordia and leaves. The shoot meristem itself was free of detectable *td1* expression (Fig. 6B). During reproductive development, weak *td1* expression was detected in the three outermost layers of the IM, and on its flanks at positions of prospective SPMs (Fig. 6C,D). The expression in the IM was always significantly lower than in the emerging SPMs. *td1* transcript levels remained high as SPMs produce SMs (Fig. 6D) and in the apex of the floral meristems in the L1, L2 and L3 layers (Fig. 6E,F). By contrast to the *CLV1* pattern (Clark et al., 1997), but similar to that of *FON1* (Suzaki et al., 2004), *td1* transcripts were detected in primordia of glumes, lemmas

and stamens (Fig. 6E,F). Thus, the *td1* RNA was not confined to meristematic cells but was also found in lateral organs of the ear, as in the vegetative shoot. *td1* expression during male inflorescence development was identical to that of the female (data not shown).

td1/fea2 double mutant analysis

CLV1 and 2 are reported to act in a common pathway in *Arabidopsis* (Kayes and Clark, 1998), and this is supported by biochemical analysis (Jeong et al., 1999). To ask whether *td1* and *fea2*, the maize orthologs of *CLV1* and *2*, respectively, act in a common pathway, we analyzed *td1/fea2* double mutants. At early stages of ear development *td1/fea2* double mutants (Fig. 7A) were strikingly similar to strong *td1* mutants (Fig. 7B), in showing a severe ring fasciation, whereas *fea2* mutant siblings were less strongly fasciated (Fig. 7C). At maturity, *td1/fea2* double mutants showed additive or synergistic phenotypes, as they initiated twice as many rows of spikelets as either *td1* or *fea2* single mutants (Table 3), and their ears were reduced in length (Fig. 7D). The decrease in leaf number was also more pronounced in *td1/fea2* double mutants compared with either single mutant (Table 3), indicating that, like *td1*, *fea2* also functions during vegetative development.

Following the assumption that ear spikelet number correlates with inflorescence meristem size, our data indicate that *td1* and *fea2* do not act exclusively in a single pathway to control meristem size.

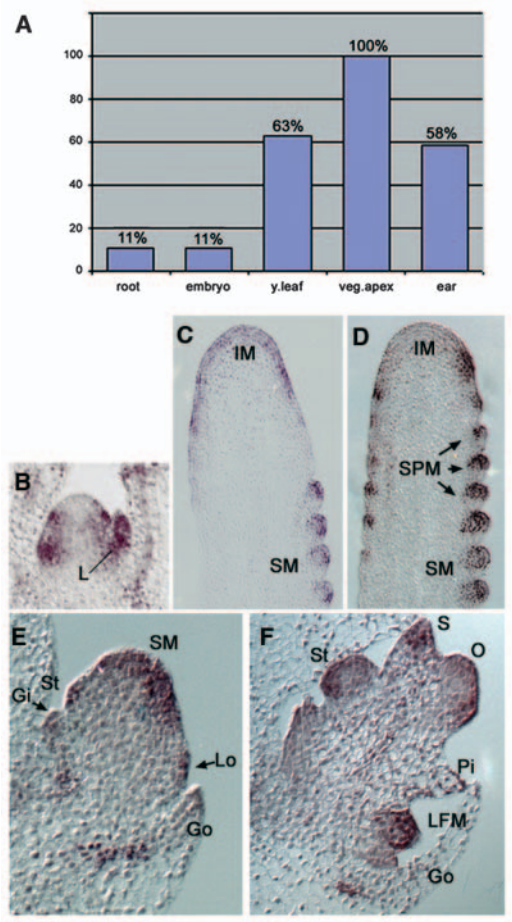

Fig. 6. Organ- and tissue-specific expression analysis of *td1*. Organ-specific analysis of *td1* transcription was carried out by quantitative real-time RT-PCR using endogenous *ubiquitin* transcript levels for normalization. Highest *td1* transcript level is detected in the vegetative apex arbitrarily set to 100%. The RNA level is lower in the female inflorescence (58%). Low *td1* transcript levels are detected in the embryo (11%) or the root (11%). A significant *td1* transcript level is also detected in young leaves (63%). (B-F) In-situ expression pattern of *td1* in shoot meristems at different stages of development. (B) Late vegetative shoot apex, showing *td1* expression in developing leaves but also absence of detectable *td1* expression in the SAM. (C) Tip of an ear primordium, showing weak *td1* expression in the three outermost layers of the IM and *td1* expression within SMs. (D) Tip of an ear primordium showing *td1* expression in adaxial parts of the emerging SPMs. (E) Developing SM (stage F), showing expression within the SM and also in developing inner and outer glume and outer lemma primordia. (F) Upper and lower floral meristem (stage H): *td1* is expressed strongly within the lower FM, but also in the developing ovule, silk and stamen primordia of the upper FM. Gi, inner glume; Go, outer glume; L, leaf; Lo, outer lemma; St, stamen primordium; S, silk primordium; O, ovule primordium; Pi, inner palea; LFM, lower floral meristem.

Discussion

The *td1* gene of maize regulated meristem size during inflorescence development. The ears showed the strongest effect, with massively fasciated tips and additional and irregular kernel rows. Tassels of *td1* mutants were also thicker, and the plants were slightly shorter, with fewer leaves. Using a combination of reverse genetics and targeted transposon tagging, we have identified the *td1* gene as an ortholog of *CLV1*. *td1* mutants were similar to *fea2* mutants, and given that *fea2* encodes a CLV2-like protein one could assume that FEA2 and TD1 may function in a common pathway, like CLV1 and

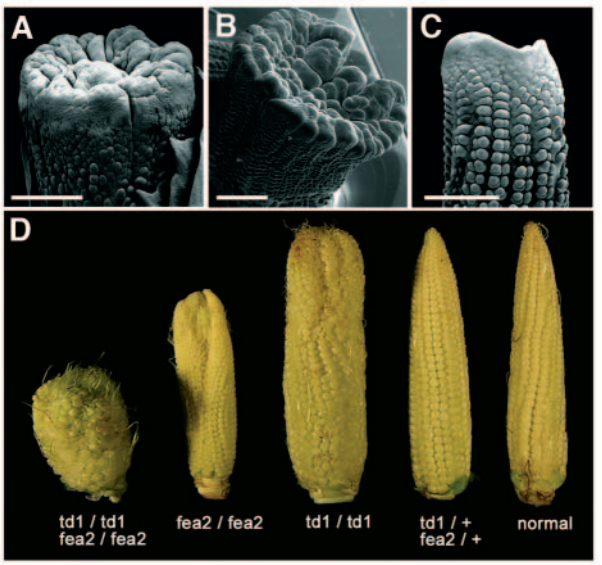

Fig. 7. Ear morphology in *td1/fea2* double mutants compared with single mutant and normal siblings. (A) SEM of a *td1/fea2* double mutant ear compared with *td1*- (B) and *fea2*- (C) single mutant ears. (D) *td1/fea2* double mutant ears exhibit an additive and synergistic phenotype as they produce more kernel rows in a highly irregular pattern (see also Table 3). In addition ears were shorter than their single mutant and normal siblings. Double heterozygote ears show no defects compared with normal siblings. Scale bars: 1 mm.

CLV2 in *Arabidopsis*. Our analysis, however, suggests that *td1* and *fea2* do not function exclusively in a single pathway, as the double mutants between the putative null alleles show some additive and synergistic phenotypes. Comparisons of the phenotypes and expression patterns revealed further similarities and differences between maize, rice and *Arabidopsis CLV1*-orthologs.

Phenotypic consequences of *td1* mutants

The most conspicuous aspect of *td1* mutants was the dramatic fasciation of the ear tip, due to an enlarged inflorescence meristem. Ear tips showed line or ring fasciation and were often bifurcated. The broadening of the tip led to extra rows of SPMs and extra SMs, which sometimes produced abnormal single spikelets. By contrast to the dramatic defect in the ear, tassels of *td1* mutants appeared less affected. However, a closer analysis showed that spikelet density was increased by about 40% in the main rachis of the tassel, but it did not fasciate. Interestingly, *kn1* null mutants reduced meristem size, and while *kn1* mutant ears and tassels shared a set of meristem defects, only in the ear did the inflorescence meristem sometimes abort, leading to plants without ears (Kerstetter et al., 1997; Vollbrecht et al., 2000). Thus, the ear appeared to be more sensitive than the tassel to mutations that alter inflorescence meristem size.

Given the similarity of ear and tassel primordia at early stages of development (Cheng et al., 1983), it is interesting to speculate on the reasons for the differences between the mature tassel and ear of *td1* mutants. One possibility is that the ear is more sensitive to changes in CLV signaling, due to the selective pressure placed on the ear during agricultural selection. Maize was domesticated from teosinte, in which the inflorescence rachis contains only a single alternating row of spikelets. By contrast, a typical maize ear contained 16-18 spikelet rows (Doebley and Stec, 1991). Evidence for a general relaxed control of meristem size in the ear also comes from the observation that it is not uncommon to find spontaneously fasciated ears, whereas such abnormalities are rare for the tassel (Neuffer et al., 1997). Interestingly, *td1* maps near the location of a quantitative trait locus (QTL) for seed row number between the markers BNL6.25 and BNL5.02 (Doebley et al., 1990) and a QTL for tassel spikelet density on tassel branches (T. Rocheford, personal communication). The rice *FON1* gene also encodes a *CLV1* ortholog (Suzaki et al., 2004), and additional branches are made in rice *fon1* inflorescences to a similar magnitude as the formation of extra spikelets in male *td1* inflorescences, suggesting that *TD1* and *FON1* bear equivalent functions. This finding again strengthens the view that the maize ear reflects a unique structure among grass species, with a distinct genetic program from the tassel, possibly as a result of the intense selective pressure during domestication.

Other meristems were also affected in *td1* mutant inflorescences. SPMs were frequently enlarged and irregularly arranged, leading to extra spikelets that were often single instead of in pairs. Although we did not observe more than two florets per spikelet, we did observe extra glumes. As glumes are products of the SM (McSteen and Hake, 2001), the SMs were therefore also affected in *td1* mutants. *td1* mutant male flowers also showed an increase in the number of stamens, which may be a consequence of an increase in floral meristem size. Finally, *td1* mutant plants were shorter and developed fewer leaves. Given that *td1* maps near a QTL for plant height (Beavis et al., 1991), it could also be responsible for natural variation in height.

In summary, *td1* functions to limit meristem size during inflorescence and flower development.

td1 encodes a CLV1-like protein

We have shown that *td1* encodes a putative ortholog of CLV1. *clv1* mutants affect all shoot meristem types, including those of the embryo and vegetative phase. With the exception of the ear inflorescence meristem, the effects of the *td1* mutation were relatively mild, and this could be a result of genetic redundancy. Although *td1* appears to be a single-copy gene by low stringency Southern hybridizations, sequence database searches indicate a plethora of LRR receptor-like genes in maize, and these could account for the genetic redundancy. From the *Arabidopsis* genome, 216 LRR-RLKs have been identified (Shiu and Bleeker, 2001), and recent studies of *clv1* dominant negative alleles strongly suggest the presence of additional receptor kinases that function redundantly with CLV1 in the *Arabidopsis* SAM (Diévart et al., 2003). Our phylogenetic analysis indicates an ancestral gene duplication prior to the divergence of monocot and dicot species, giving rise to two discrete branches. *CLV1*, *FON1* and *TD1* fall into subfamily A, whereas the three maize kinases encoded by *ZmKin1* to *3* fall into subfamily B, along with *OsLRK1* from rice and the two *Arabidopsis* LRR-RLKs, *A.t. RLK1* and *A.t. RLK2*. Interestingly, *OsLRK1* antisense plants have an increased number of floral organs, implicating a function in control of floral meristem size (Kim et al., 2000). The presence of *A.t. RLK1* and *2* in the same subfamily (B) indicates that redundancy presumably is ancient and these two genes still may act redundantly to *CLV1* in *Arabidopsis*.

TD1 and FEA2 do not interact in an exclusive receptor complex

The *td1* mutant phenotype was similar to that of *fea2*, which also has ear fasciation, an increased number of stamens, and a thicker tassel. FEA2 is predicted to be a CLV2 ortholog (Taguchi-Shiobara et al., 2001). In *Arabidopsis*, the *CLV1* and *CLV2* gene products interact to form a heterodimeric LRR-transmembrane receptor kinase complex [reviewed by Sharma et al. (Sharma et al., 2003a)], and this is supported by genetic analysis that shows that strong *clv1* and *clv3* alleles are epistatic to *clv2* in regulating meristem size (Kayes and Clark, 1998). Given the similar phenotypes of *fea2* and *td1* mutants, it is intriguing to speculate whether they encode two subunits of a heterodimeric *CLV*-like LRR-receptor kinase complex in maize.

Our analysis of *td1/fea2* double mutants, however, indicates that the situation in maize is more complex. The formation of twice as many kernel rows, as well as the enhanced reduction of leaf number, in *td1/fea2* double mutants compared with either single mutant strongly suggests that *td1* and *fea2* do not simply function in a single pathway, for example as an exclusive receptor-co-receptor complex. One could speculate that *td1* and *fea2* are incorporated into different receptor complexes, thereby acting in independent pathways in regulating shoot and inflorescence meristem size. Alternatively, they may function in partially overlapping

pathways, for example forming a co-receptor complex as well as dimerizing with other LRR partners, as has been also recently proposed for CLV1 function in *Arabidopsis* (Diévart et al., 2003). Our data suggest that several CLV1-CLV2-like complexes with partially redundant functions contribute to the regulation of inflorescence meristem size, and that the degree of redundancy may differ in the ear and tassel. As there are multiple *CLV3*-like genes in maize (Cock and McCormick, 2001; Sharma et al., 2003b), further specificity may be dictated by specific ligand-receptor interactions.

The CLV1 and TD1 protein structures are highly conserved. Like CLV1 (Clark et al., 1997), the extracellular receptor domain of TD1 is composed of 21 complete LRR motifs, each of 23-25 amino acids in length. These LRR motifs are commonly used for protein-protein interactions (Kobe and Deisenhofer, 1994; Kobe and Deisenhofer, 1995) and all motifs in TD1, as in CLV1, belong to the LRR-XI subfamily (Shiu and Bleeker, 2001). Sequence analyses of strong *clv1* alleles in *Arabidopsis* reveal lesions within LRRs four, five or nine, implying these regions may be important for ligand specifity (Diévart et al., 2003). Interestingly, sequence similarity between TD1 and CLV1 is more pronounced within LRR-5 and LRR-9, supporting the hypothesis that these LRRs play a conserved role in the receptor-ligand interaction. This situation is reminiscent of the FEA2 and CLV2 proteins, which also show blocks of significant similarity in specific LRRs (Taguchi-Shiobara et al., 2001).

Another common feature of LRR-RLKs are paired cysteines flanking the extracellular LRR domain. These cysteines are implicated in receptor dimerization (Trotochaud et al., 1999). TD1, FON1 and CLV1 share both cysteine pairs, although the spacing of the carboxy terminal cysteines is only two amino acid residues in TD1 relative to six in CLV1 and seven in FON1. Interestingly, in FEA2 the carboxy terminal cysteine pairs are also closer together, spaced by only four amino acids, compared with seven in CLV2 (Taguchi-Shiobara et al., 2001; Jeong et al., 1999). Therefore, TD1 and FEA2 contain putative compensatory alterations that might stabilize heterodimers by intermolecular disulfide bridges, via the carboxy terminal pair of cysteines.

Expression analysis shows a potentially wider role for *td1* compared with *CLV1*

Significant differences in expression pattern can be found between *TD1* in maize and *CLV1* in *Arabidopsis*. *td1* expression was not restricted to the internal L2/L3 meristem layers, as reported for *CLV1* (Clark et al., 1997). Furthermore, similar to the *FON1* expression in rice, *td1* was expressed in inflorescence organ primordia, such as glumes, lemma and stamens, whereas *CLV1* is expressed only in meristems. More significantly, we did not observe *td1* expression in the shoot apical meristem of embryos or seedlings using in-situ hybridizations. One explanation for the lack of detection at the cellular level, however, is a ubiquitous but low level of expression in embryonic or seedling shoot meristems.

An interpretation of the low level of *td1* expression in the ear inflorescence meristem again takes the domestication of maize into consideration. The change in phyllotaxy and increase in spikelet row number during selection for maize ear size may have been accompanied by an increase in inflorescence meristem size, by modification of genetic pathways, such as the *CLV* pathway. In other words, selection for low *td1* expression in the ear inflorescence meristem may be responsible for the large size of the ear inflorescence meristem.

An alternative hypothesis is that SPMs, which express high levels of *td1* mRNA, regulate the size of the inflorescence meristem by a long-distance signaling mechanism. An interaction between inflorescence and axillary meristem is also seen with *barren inflorescence2* (*bif2*) mutants, which do not develop axillary meristems and exhibit fasciated inflorescence meristems (McSteen and Hake, 2001). *bif2* is also expressed in axillary meristems but not in the inflorescence meristem (McSteen and Hake, unpublished). The same scenario can also be postulated for the vegetative shoot meristem, as *td1* is expressed in leaves.

Conclusion

In summary, the *td1* fasciated and enlarged meristem phenotypes are explained by a deficiency in CLV-type signaling. The finding that *td1* and *FON1* encode orthologs of *CLV1* supports the notion that the regulation of stem cell proliferation by CLV-type signaling is of general importance in plants. However, our data point out important differences that justify the study of such pathways in a variety of model systems. For example, *td1* expression was not detected, or was very weak, in vegetative and inflorescence apical meristems, and analysis of *td1/ fea2* mutant plants indicated that *td1* and *fea2* do not exclusively act in a simple co-receptor complex. Moreover, the proximity between *td1* and QTLs affecting seed row number, spikelet density and plant height suggests that CLV signaling may have been a target of selection during domestication of maize as a crop. Our results suggest that genes such as *td1* could be manipulated to improve crop yields.

The authors thank R. Waites for inspiring discussions and technical assistance at the start of the project, and J. Chandler and S. Dass for critically reading the manuscript. Thanks to T. Rocheford for growing out the *td1* transposon screens in Illinois and for aid in mapping *td1* relative to his floral QTLs, and to J. Lam, M. Rezapour and B. Bart for plant measurements and statistical analysis. P.B., J.N. and W.W. were supported by QLK3-2000-00196 and QLRT-2000-00302. S.H., C.L., E.V., D.J. and M.R. were supported by NSF BDI-0110189 and the USDA-ARS. P.B. and D.J. were also supported by the National Research Initiative of the USDA Cooperative State Research, Education and Extension Service, grant number #2003-35304-02625.

References

Abbe, E. C. and Stein, O. L. (1954). The growth of the shoot apex in maize: embryogeny. *Am. J. Bot.* **41**, 285-293.

Barton, M. K. and Poethig, R. S. (1993). Formation of the shoot apical meristem in *Arabidopsis thaliana*: an analysis of development in the wildtype and *SHOOTMERISTEMLESS* mutant. *Development* **119**, 823-831.

Beadle, G. W. (1980). The ancestry of corn. *Sci. Am.* **242**, 112-119.

Beavis, W. D., Grant, D., Albertsen, M. C. and Fincher, R. R. (1991). Quantitative trait loci for plant height in four maize populations and their associations with qualitative genetic loci. *Theor. Appl. Genet.* **83**, 141-145.

Blauth, S. L., Jeffery, Y. Y., Klucinec, D., Shannon, J. C., Thompson, D. B. and Guilitinan, M. D. (2001). Identification of *Mutator* Insertional Mutants of Starch-Branching Enzyme 2a in Corn. *Plant Physiol.* **125**, 1396-1405.

Brand, U., Fletcher, J. C., Hobe, M., Meyerowitz, E. M. and Simon, R. (2000). Dependence of stem cell fate in *Arabidopsis* on a feedback loop regulated by CLV3 activity. *Science* **289**, 617-619.

Burr, B., Burr, F. A., Thompson, K. H., Albertson, M. C. and Stuber, C.

W. (1988). Gene mapping with recombinant inbreds in maize. *Genetics* **118**, 519-526.

Cheng, P. C., Greyson, R. I. and Walden, D. B. (1983). Organ initiation and the development of unisexual flowers in the tassel and ear of *Zea mays*. *Amer. J. Bot.* **70**, 450-462.

Clark, S. E., Running, M. P. and Meyerowitz, E. M. (1993). *CLAVATA1*, a regulator of meristem and flower development in *Arabidopsis*. *Development* **119**, 397-418.

Clark, S. E., Running, M. P. and Meyerowitz, E. M. (1995). *CLAVATA3* is a specific regulator of shoot and floral meristem development affecting the same processes as *CLAVATA1*. *Development* **121**, 2057-2067.

Clark, S. E., Jacobsen, S. E., Levin, J. Z. and Meyerowitz, E. M. (1996). The *CLAVATA* and *SHOOTMERISTEMLESS* loci competitively regulate meristem activity in *Arabidopsis*. *Development* **122**, 1567-1575.

Clark, S. E., Williams, R. W. and Meyerowitz, E. M. (1997). The *CLAVATA1* gene encodes a putative receptor kinase that controls shoot and floral meristem size in *Arabidopsis*. *Cell* **89**, 575-585.

Cock, J. M. and McCormick, S. (2001). A Large Family of Genes That Share Homology with *CLAVATA3*. *Plant Physiol.* **126**, 939-942.

Diévart, A., Dalal, M., Tax, F. E., Lacey, A. D., Huttly, A., Li, J. and Clark, S. E. (2003). *CLAVATA1* dominant-negative alleles reveal functional overlap between multiple receptor kinases that regulate meristem and organ development. *Plant Cell* **15**, 1198-1211.

Doebley, J. (1992). Mapping the genes that made maize. *Trends Genet.* **9**, 302-307.

Doebley, J. and Stec, A. (1991). Genetic analysis of the morphological differences between maize and teosinte. *Genetics* **129**, 285-295.

Doebley, J., Stec, A., Wendel, J. and Edwards, M. (1990). Genetic and morphological analysis of a maize-teosinte F2 population: implications for the origin of maize. *Proc. Natl. Acad. Sci. USA* **87**, 9888-9892.

Emerson, R. A. (1912). Inheritance of certain "abnormalities" in maize. *Am. Breed. Assoc. Rept.* **8**, 385-399.

Endrizzi, K., Moussian, B., Haecker, A., Levin, J. Z. and Laux, T. (1996). The *SHOOT MERISTEMLESS* gene is required for maintenance of undifferentiated cells in *Arabidopsis* shoot and floral meristems and acts at a different regulatory level than the meristem genes *WUSCHEL* and *ZWILLE*. *Plant J.* **10**, 101-113.

Fletcher, J. C., Brand, U., Running, M. P., Simon, R. and Meyerowitz, E. M. (1999). Signaling of cell fate decisions by *CLAVATA3* in *Arabidopsis* shoot meristems. *Science* **283**, 1911-1914.

Galinat, W. C. and Naylor, A. W. (1951). Relation of photoperiod to inflorescence proliferation in *Zea mays*. *Am. J. Bot.* **38**, 38-47.

Hanks, S. K. and Quinn, A. M. (1991). Protein-kinase catalytic domain sequence database: identification of conserved features of primary structure and classification of family members. *Methods Enzymol.* **200**, 38-62.

Jackson, D. and Hake, S. (1999). The genetics of ear fasciation in maize. *Maize Newsletters* **73**, 2.

Jackson, D., Veit, B. and Hake, S. (1994). Expression of maize *knotted1*-related homeobox genes in the shoot apical meristem predicts patterns of morphogenesis in the vegetative shoot. *Development* **120**, 405-413.

Jeong, S., Trotochaud, A. E. and Clark, S. E. (1999). The *Arabidopsis CLAVATA2* gene encodes a receptor-like protein required for the stability of the *CLAVATA1* receptor-like kinase. *Plant Cell* **11**, 1925-1934.

Kayes, J. M. and Clark, S. E. (1998). *CLAVATA2*, a regulator of meristem and organ development in *Arabidopsis*. *Development* **125**, 3843-3851.

Kellogg, E. and Birchler, J. (1993). Linking phylogeny and genetics: *Zea mays* as a tool for phylogenetic studies. *Syst. Biol.* **42**, 435-439.

Kerstetter, R. A. and Hake, S. (1997). Shoot meristem formation in vegetative development. *Plant Cell* **9**, 1001-1010.

Kerstetter, R. A., Laudencia-Chingcuanco, D., Smith, L. G. and Hake, S. (1997). Loss of function mutations in the maize homeobox gene, *knotted1*, are defective in shoot meristem maintenance. *Development* **124**, 3045-3054.

Kim, C. H., Jeong, D. H. and An, G. H. (2000). Molecular cloning and characterization of OsLRK1 encoding a putative receptor-like protein kinase from *Oryza sativa*. *Plant Sci.* **152**, 17-26.

Kobe, B. and Deisenhofer, J. (1994). The leucine-rich repeat. A versatile binding motif. *Trends Biochem. Sci.* **19**, 415-421.

Kobe, B. and Deisenhofer, J. (1995). A structural basis of the interactions between leucine-rich repeats and protein ligands. *Nature* **37**, 183-186.

Kumar, S., Tamura, K., Jakobsen, I. B. and Masatoshi Nei, M. (2001). *MEGA2: Molecular Evolutionary Genetics Analysis Software*. *Biochemistry* **17**, 1244-1245.

Laux, T., Mayer, K. F., Berger, J. and Juergens, G. (1996). The *WUSCHEL* gene is required for shoot and floral meristem integrity in *Arabidopsis*. *Development* **122**, 87-96.

Long, J. A., Moan, E. I., Medford, J. I. and Barton, M. K. (1996). A member of the KNOTTED class of homeodomain proteins encoded by the SHOOTMERISTEMLESS gene of *Arabidopsis*. *Nature* **379**, 66-69.

Luckwill, L. C. (1943). The evolution of the cultivated tomato. *Jour. Royal Hort. Soc.* **68**, 19-25.

Lunde, C. F., Morrow, D. J., Roy, L. M. and Walbot, V. (2003). Progress in maize gene discovery: a project update. *Funct. Integr. Genomics* **31-2**, 25-32.

Mayer, K. F., Schoof, H., Haecker, A., Lenhard, M., Jurgens, G. and Laux, T. (1998). Role of *WUSCHEL* in regulating stem cell fate in the *Arabidopsis* shoot meristem. *Cell* **95**, 805-815.

McSteen, P. and Hake, S. (2001). *barren inflorescence2* regulates axillary meristem development in the maize inflorescence. *Development* **128**, 2881-2891.

McSteen, I., Laudencia-Chingcuanco, I. and Colasanti, I. (2000). A floret by any other name: control of meristem identity in maize. *Trends Plant Sci.* **5**, 61-66.

Neuffer, M. G., Coe, E. H. and Wessler, S. R. (1997). *Mutants of Maize*. 2nd edn. Plainview, New York: Cold Spring Harbor Laboratory Press.

Orr, A. R., Haas, G. and Sundberg, M. D. (1997). Organogenesis of *fascicled* ear mutant inflorescences in maize (Poaceae). *Am. J. Bot.* **84**, 723-734.

Piperno, D. R. and Flannery, R. V. (2001). The earliest archaeological maize (Zea mays L.) from highland Mexico: new accelerator mass spectrometry dates and their implications. *Proc. Natl. Acad. Sci. USA* **98**, 2101-2103.

Robertson, D. S. (1978). Characterization of a *Mutator* system in maize. *Mutat. Res.* **51**, 21-28.

Rojo, E., Sharma, V. K., Kovaleva, V., Raikhel, N. V. and Fletcher, J. C. (2002). CLV3 is localized to the extracellular space, where it activates the *Arabidopsis* CLAVATA stem cell signaling pathway. *Plant Cell* **14**, 969-977.

Schoof, H., Lenhard, M., Haecker, A., Mayer, K. F., Jurgens, G. and Laux, T. (2000). The stem cell population of *Arabidopsis* shoot meristems in maintained by a regulatory loop between the CLAVATA and *WUSCHEL* genes. *Cell* **100**, 635-644.

Sharma, V. K., Carles, C. and Fletcher, J. C. (2003a). Maintenance of stem cell populations in plants. *Proc. Natl. Acad. Sci. USA* **100**, 11823-11829.

Sharma, V. K., Ramirez, J. and Fletcher, J. C. (2003b). The Arabidopsis *CLV3*-like genes are expressed in diverse tissues and encode secreted proteins. *Plant Mol. Biol.* **51**, 415-425.

Shiu, S. H. and Bleecker, A. B. (2001). Plant receptor-like kinase gene family: diversity, function, and signaling. *Sci. STKE* **2001**, RE22.

Smith, L. G., Greene, B., Veit, B. and Hake, S. (1992). A dominant mutation in the maize homeobox gene, *knotted1*, causes its ectopic expression in leaf cells with altered fates. *Development* **116**, 21-30.

Sommer, H., Beltran, J. P., Huijser, P., Pape, H., Lonnig, W. E., Saedler, H. and Schwarz-Sommer, Z. (1990). Deficiens, a homeotic gene involved in the control of flower morphogenesis in *Antirrhinum majus*: the protein shows homology to transcription factors. *EMBO J.* **9**, 605-613.

Steeves, T. A. and Sussex, I. M. (1989). Patterns in Plant Development. Cambridge, UK: Cambridge University Press.

Suzaki, T., Sato, M., Ashikari, M., Miyoshi, M., Nagato, Y. and Hirano, H. Y. (2004). The gene FLORAL ORGAN NUMBER1 regulates floral meristem size in rice and encodes a leucine-rich repeat receptor kinase orthologous to Arabidopsis CLAVATA1. *Development* **131**, 5649-5657.

Taguchi-Shiobara, F., Yuan, Z., Hake, S. and Jackson, D. (2001). The *fasciated ear2* gene encodes a leucine-rich repeat receptor-like protein that regulates shoot meristem proliferation in maize. *Genes Dev.* **15**, 2755-2766.

Trotochaud, A. E., Hao, T., Wu, G., Yang, Z. and Clark, S. E. (1999). The *CLAVATA1* receptor-like kinase requires *CLAVATA3* for its assembly into a signaling complex that includes KAPP and a Rho-related protein. *Plant Cell* **11**, 393-406.

Vollbrecht, E., Reiser, L. and Hake, S. (2000). Shoot meristem size is dependent on inbred background and presence of the maize homeobox gene, *knotted1*. *Development* **127**, 3161-3172.

Zielinski, Q. (1945). Fasciation in horticultural plants with special reference to the tomato. *Proc. Am. Hort. Sci.* **46**, 263-268.